

EFFECTS OF SPECULAR REFLECTION ON RADIATIVE HEAT TRANSFER IN AN ABSORBING, EMITTING, AND ANISOTROPICALLY-SCATTERING MEDIUM

W. W. YUEN and L. W. WONG

Department of Mechanical and Environmental Engineering, University of California, Santa Barbara,
CA 93106, U.S.A.

(Received 19 September 1980)

Abstract—The effect of specular reflection in a one-dimensional, absorbing, emitting, and anisotropically-scattering medium is analyzed. The mathematical formulation is shown to involve the function $F_n(x) = \int_0^1 (e^{-x\mu} / 1 - \rho_1 \rho_2 e^{-2L\mu}) \mu^{n-2} d\mu$, which can be readily evaluated as a fast-converging, infinite series of exponential integral functions. Numerical solutions to the resulting integral equations are generated by the method of point allocation.

Physically, the radiative energy within a participating medium bounded by specularly reflective surfaces is observed to experience more multiple reflection than the corresponding diffuse reflection case. This leads to some differences between the two cases in the heat transfer and temperature profile results. These differences, however, are generally quite minor for the considered one-dimensional planar system.

1. INTRODUCTION

Radiative heat transfer in an absorbing, emitting, and scattering medium is a problem of considerable practical importance. A great deal of work has been reported in this area during recent years.¹⁻⁴ With few exceptions,⁵⁻⁷ most of these studies assumed that the boundary of the enclosure considered is a diffusely emitting and reflecting surface. While this assumption can probably be considered as an accurate description for some selected surfaces, many real surfaces emit diffusely but reflect specularly. For practical applications it is, therefore, important that the effect of specular reflection on the radiative heat transfer in a participating medium is clearly understood.

Currently, quantitative studies on the effect of specular reflection on radiative heat transfer are quite limited. Cess and Sotak⁵ obtained solutions for a one-dimensional planar medium under condition of radiative equilibrium with no internal heat generation. However, to reduce the mathematical complexity they made a restrictive assumption that one of the two boundary surfaces is black. The effect of scattering was also neglected in their analysis. Pao⁶ and Ozisik and Siewert⁷ developed different methods of solution for the equation of transfer in a parallel slab with specularly reflecting boundary. In both of these studies energy conservation was not considered and a temperature distribution in the medium is assumed. These results thus have only limited applicability in heat-transfer calculations.

The objective of this work is to assess quantitatively the general effect of specular reflection on radiative heat transfer. A one-dimensional planar system, in which both boundaries are specularly reflecting and diffusely emitting, will be considered. The equations for radiative transfer and energy conservation will be solved simultaneously. Anisotropic scattering and internal heat generation will be included in the analysis. Based on these results, the effects of specular reflection on the temperature profile of the medium and heat transfer will be determined and discussed.

2. MATHEMATICAL FORMULATION

The physical model and the associated coordinate system are identical to those in previous work.¹⁻³ Briefly, the medium is assumed to be gray, absorbing, emitting, and scattering anisotropically according to the following phase function

$$p(\cos \theta_0) = 1 + x \cos \theta_0, \quad -1 \leq x \leq 1, \quad (1)$$

where θ_0 is the angle between the incoming and the scattering ray and x the forward-backward scattering parameter. The transfer equation becomes

$$\mu \frac{di}{d\tau} + i = (1 - \omega_0)i_b + \frac{\omega_0}{4\pi} G(\tau) = \frac{\omega_0 x \mu}{4\pi} q(\tau) \quad (2)$$

with

$$G(\tau) = 2\pi \int_{-1}^1 i \, d\mu \quad (3)$$

and

$$q(\tau) = 2\pi \int_{-1}^1 i\mu \, d\mu. \quad (4)$$

In the above equations, i stands for the radiative intensity, i_b the blackbody intensity, ω_0 the scattering albedo, $\mu = \cos \theta$, and τ the optical coordinate defined by $d\tau = \beta \, dz$ with z being the spatial coordinate and β the extinction coefficient. Assuming that the optical coordinates of the two boundaries are $\tau = -L/2$ and $\tau = L/2$, respectively, where L is the optical thickness of the one-dimensional system, the boundary conditions for diffuse emission and specular reflection at the two surfaces are

$$i_1(\mu) = i\left(-\frac{L}{2}, \mu\right) = \epsilon_1 \frac{\sigma T_1^4}{\pi} + \rho_1 i\left(-\frac{L}{2}, -\mu\right), \quad 0 \leq \mu \leq 1, \quad (5)$$

$$i_2(\mu) = i\left(\frac{L}{2}, \mu\right) = \epsilon_2 \frac{\sigma T_2^4}{\pi} + \rho_2 i\left(\frac{L}{2}, -\mu\right), \quad -1 \leq \mu \leq 0, \quad (6)$$

with ϵ_1 , T_1 and ϵ_2 , T_2 being the emissivities and temperatures at the two surfaces and $\rho_1 = (1 - \epsilon_1)$, $\rho_2 = (1 - \epsilon_2)$ the reflectivities. Finally, the energy equation is given by

$$dq/d\tau = S/\beta, \quad (7)$$

where S is the internal heat generation rate.

Equations (2) and (7), together with the definition of q given by Eq. (4), can be combined in the standard manner to yield the following expressions for the radiative intensity:

$$i(\mu, \tau) = i_1(\mu) e^{-[(L/2)+\tau]/\mu} + \frac{1}{4\pi} \int_{-(L/2)}^{\tau} H(\mu, \tau^*) e^{-(\tau-\tau^*)/\mu} \frac{d\tau^*}{\mu}, \quad 0 \leq \mu \leq 1, \quad (8)$$

$$i(\mu, \tau) = i_2(\mu) e^{[(L/2)-\tau]/\mu} - \frac{1}{4\pi} \int_{\tau}^{L/2} H(\mu, \tau^*) e^{(\tau^*-\tau)/\mu} \frac{d\tau^*}{\mu}, \quad -1 \leq \mu \leq 0, \quad (9)$$

where

$$H(\mu, \tau) = G(\tau) + \omega_0 x \mu q(\tau) + S/\beta. \quad (10)$$

Substituting Eqs. (8) and (9) into Eqs. (3) and (4), a set of coupled integral equations for $G(\tau)$ and $q(\tau)$ can be generated. As in Ref. 8, these equations may be simplified in canonical form by first introducing the following transformations:

$$G(\tau) = 4\sigma T_2^4 + \sigma(T_1^4 - T_2^4)g_i(\tau) + \sigma S g_s(\tau), \quad (11)$$

$$q(0) = (\sigma T_1^4 - \sigma T_2^4)q_{i0} + q_{s0}. \quad (12)$$

Physically, $g_i(\tau)$ and q_{i0} stand for the dimensionless temperature profile and centerpoint heat flux for the case of unequal wall temperature and no heat generation; $g_s(\tau)$ and q_{s0} , on the other hand, are values for the case with equal wall temperature and non-zero uniform internal heat generation.

The integral equation for $g_i(\tau)$ is

$$g_i(\tau) = 2\epsilon_1 F_2\left(\frac{L}{2} + \tau\right) + 2\epsilon_1 \rho_2 F_2\left(\frac{3L}{2} - \tau\right) + 2\epsilon_1 U(\tau) F_3\left(\frac{L}{2}\right) - 2\epsilon_1 \rho_2 U(\tau) F_3\left(\frac{3L}{2}\right) + \Psi[g_i(\tau)], \quad (13)$$

where $F_n(x)$ is a function originally introduced by Cess and Sotak⁵ as

$$F_n(x) = \int_0^1 \frac{e^{-x/\mu}}{1 - \rho_1 \rho_2 e^{-2L/\mu}} \mu^{n-2} d\mu \quad (14)$$

and $U(\tau)$ is given by

$$U(\tau) = \frac{\omega_0 x \left[(1 + \rho_2) \left[\rho_1 F_3\left(\frac{3L}{2} + \tau\right) + F_3\left(\frac{L}{2} - \tau\right) \right] - (1 + \rho_1) \left[\rho_2 F_3\left(\frac{3L}{2} - \tau\right) + F_3\left(\frac{L}{2} + \tau\right) \right] \right]}{2 - \omega_0 x \left[\frac{2}{3} + (2\rho_1 \rho_2 + \rho_1 + \rho_2) F_4\left(\frac{3L}{2}\right) - (2 + \rho_1 + \rho_2) F_4\left(\frac{L}{2}\right) \right]}, \quad (15)$$

$\Psi[g_i(\tau)]$ is an integral operator on $g_i(\tau)$ which can be written as

$$\begin{aligned} \Psi[g_i(\tau)] = & \frac{1}{2} \int_{-(L/2)}^{L/2} g_i(\tau^*) E_1(\tau - \tau^*) d\tau^* - \frac{U(\tau)}{2} \int_0^{L/2} [g_i(\tau^*) - g_i(-\tau^*)] \\ & \times E_2(\tau^*) d\tau^* + \frac{\rho_1 \rho_2}{2} \int_{-(L/2)}^{L/2} g_i(\tau^*) M(L, \tau, \tau^*) d\tau^* + \frac{\rho_1}{2} \int_{-(L/2)}^{L/2} g_i(\tau^*) \\ & \times [F_1(L + \tau + \tau^*) + U(\tau) F_2(L + \tau^*)] d\tau^* + \frac{\rho_2}{2} \int_{-(L/2)}^{L/2} g_i(\tau^*) \\ & \times [F_1(L - \tau - \tau^*) + U(\tau) F_2(L - \tau^*)] d\tau^*, \end{aligned} \quad (16)$$

with $E_n(\tau)$ being the exponential integral function and

$$M(L, \tau, \tau^*) = F_1(2L + \tau - \tau^*) + F_1(2L - \tau + \tau^*) + U(\tau)[F_2(2L - \tau^*) - F_2(2L + \tau^*)]. \quad (17)$$

After $g_i(\tau)$ is determined from Eq. (13), q_{i0} becomes

$$q_{i0} = \frac{2\epsilon_1 F_3\left(\frac{L}{2}\right) - 2\epsilon_1 \rho_2 F_3\left(\frac{3L}{2}\right) + \Phi(g_i(\tau))}{1 - \frac{\omega_0 x}{2} \left[\frac{2}{3} + (2\rho_1 \rho_2 + \rho_1 + \rho_2) F_4\left(\frac{3L}{2}\right) - (2 + \rho_1 + \rho_2) F_4\left(\frac{L}{2}\right) \right]}. \quad (18)$$

with the operator Φ defined by

$$\begin{aligned} \Phi(g_i(\tau)) = & \frac{1}{2} \int_0^{L/2} [g_i(-\tau^*) - g_i(\tau^*)] E_2(\tau^*) d\tau^* + \frac{\rho_1 \rho_2}{2} \int_{-(L/2)}^{L/2} g_i(\tau^*) [F_2(2L - \tau^*) \\ & - F_2(2L + \tau^*)] d\tau^* + \frac{\rho_1}{2} \int_{-(L/2)}^{L/2} g_i(\tau^*) F_2(L + \tau^*) d\tau^* \\ & - \frac{\rho_2}{2} \int_{-(L/2)}^{L/2} g_i(\tau^*) F_2(L - \tau^*) d\tau^*; \end{aligned} \quad (19)$$

$g_S(\tau)$, on the other hand, can be shown to satisfy the following integral equation:

$$\begin{aligned} g_S(\tau) = & 4 \left(1 - \frac{\omega_0 x}{3} \right) [1 - U(\tau)\tau] - 2\epsilon_1 \left[M_2 \left(\frac{L}{2}, \tau \right) + \rho_2 N_2 \left(\frac{3L}{2}, \tau \right) \right. \\ & - \omega_0 x \left[M_4 \left(\frac{L}{2}, \tau \right) - \rho_2 N_4 \left(\frac{3L}{2}, \tau \right) \right] - 2\epsilon_2 \left[N_2 \left(\frac{L}{2}, \tau \right) + \rho_1 M_2 \left(\frac{3L}{2}, \tau \right) - \omega_0 x \left[N_4 \left(\frac{L}{2}, \tau \right) \right. \right. \\ & - \rho_1 M_4 \left(\frac{3L}{2}, \tau \right) \left. \right] + \omega_0 x L \left[(1 + \rho_1) \left[M_3 \left(\frac{L}{2}, \tau \right) + \rho_2 N_3 \left(\frac{3L}{2}, \tau \right) \right] \right. \\ & \left. \left. + (1 + \rho_2) \left[N_3 \left(\frac{L}{2}, \tau \right) + \rho_1 M_3 \left(\frac{3L}{2}, \tau \right) \right] \right] + \Psi(g_S(\tau)) \end{aligned} \quad (20)$$

with

$$M_i(x, y) = F_i(x + y) + U(y)F_{i+1}(x + y), \quad (21)$$

$$N_i(x, y) = F_i(x - y) - U(y)F_{i+1}(x - y); \quad (22)$$

also,

$$q_{S0} = \frac{(\epsilon_2 - \epsilon_1) \left[F_3 \left(\frac{L}{2} \right) - F_3 \left(\frac{3L}{2} \right) + \omega_0 x \left[F_5 \left(\frac{3L}{2} \right) - F_5 \left(\frac{L}{2} \right) + \frac{L}{2} F_4 \left(\frac{L}{2} \right) + \frac{L}{2} F_4 \left(\frac{3L}{2} \right) \right] \right] + \Phi(g_S(\tau))}{1 - \frac{\omega_0 x}{2} \left[\frac{2}{3} + (2\rho_1\rho_2 + \rho_1 + \rho_2)F_4 \left(\frac{3L}{2} \right) - (2 + \rho_1 + \rho_2)F_4 \left(\frac{L}{2} \right) \right]}$$

Equations (13), (18), (20), and (23) constitute the complete set of governing equations for the considered problem.

3. METHOD OF SOLUTION

While exact analytical solution to Eqs. (13) and (20) are difficult to obtain, numerical and approximate solutions are quite straightforward. The integral function $F_n(x)$, which is unique to the problem with specular reflection, can be readily tabulated by first expanding it into a series of exponential integral functions as follows:

$$F_n(x) = \sum_{k=0}^{\infty} (\rho_1\rho_2)^k E_n(x + 2kL) \quad (24)$$

Since $\rho_1\rho_2 < 1$ and $E_n(x) \rightarrow 0$ as $x \rightarrow \infty$, the above summation converges quickly for all non-zero values of ρ_1 , ρ_2 , and L .

A popular approximation approach to the present problem is the kernel substitution technique. Making the usual assumption that⁹

$$E_2(x) = \frac{3}{4} \exp \left(-\frac{3}{2}x \right), \quad (25)$$

Eq. (24), with $n = 2$ is reduced to

$$F_2(x) = \frac{3}{4} \frac{e^{-(3x/2)}}{1 - \rho_1\rho_2 e^{-3L}}. \quad (26)$$

Values for other exponential integral functions $E_n(s)$ and $F_n(x)$ ($n \geq 3$) can be readily generated from the following recursive relations:

$$\frac{d}{dx} (E_n(x)) = -E_{n-1}(x) \quad (27)$$

and

$$\frac{d}{dx}(F_n(x)) = -F_{n-1}(x). \quad (28)$$

Substituting Eqs. (25) and (26) into Eqs. (13) and (20) and carrying out the usual algebraic manipulation⁹ yields results identical to those with diffusely reflecting boundary.⁹ Hence, within the framework of the exponential kernel approximation, diffuse reflection and specular reflection yield identical heat-transfer result. It is interesting to note that this same conclusion, for cases without scattering and one black boundary, was also reached in Ref. 5.

Numerically, solutions to Eqs. (13) and (20) are generated by the method of point allocation. The accuracy and convergence of this method have already been demonstrated in previous work.² Briefly, the unknown functions $g_i(\tau)$ and $g_s(\tau)$ are first expanded as polynomials as follows:

$$g_i(\tau) = \sum_{i=1}^N X_i \tau^{i-1}, \quad (29)$$

$$g_s(\tau) = \sum_{i=1}^N Y_i \tau^{i-1}. \quad (30)$$

Substituting Eqs. (29) and (30) into Eqs. (13) and (20), respectively, and evaluating N discrete points across the one-dimensional domain, two systems of N linear equations with N unknowns are generated. It can be shown that all matrix elements are expressible in terms of $E_n(x)$ and $F_n(x)$ and can thus be readily evaluated. For each N , solutions to $g_i(\tau)$ and $g_s(\tau)$ are generated with little effort.

Computational results show that these numerical solutions converge quickly as N increases. For all of the cases considered in the present work, the maximum value of N at which convergence is achieved is less than 19 [convergence is defined by requiring that the N th order solutions for $g_i(\tau)$ and $g_s(\tau)$ at ten equidistant points in the medium agree with the $(N-1)$ th solution to the third decimal place]. For systems with small optical thickness ($L < 1.0$), the values of N required for convergence is actually much less.

4. RESULTS AND DISCUSSION

To demonstrate the effect of specular reflection, the present results are now compared with those generated with diffusely reflecting boundary. The diffuse reflection results used in the comparison are obtained algebraically from the black results ($\epsilon_1 = \epsilon_2 = 1.0$) by the technique developed in Ref. 8, which is clearly applicable for the present considerations which include the effect of anisotropic scattering.

It is also interesting to note that not all values of ϵ_1 and ϵ_2 need to be considered in the comparison. From symmetry considerations, it can be readily shown that

$$G(\tau; \epsilon_1, \epsilon_2, T_1, T_2) = G(-\tau; \epsilon_2, \epsilon_1, T_2, T_1), \quad (31)$$

$$q(\tau; \epsilon_1, \epsilon_2, T_1, T_2) = q(-\tau; \epsilon_2, \epsilon_1, T_2, T_1). \quad (32)$$

In the present study, we therefore will consider only cases with $\epsilon_1 < \epsilon_2$.

The specular and diffuse reflection results for q_{i0} and q_{s0} are presented and compared in Tables 1 and 2. As expected, differences between the two results are relatively minor. Nevertheless, the specular reflection results for q_{i0} and q_{s0} are smaller than the corresponding diffuse reflection values for all cases. Physically, these results can be explained by noting that, with a participating medium, radiant energy undergoes more multiple reflection in a system with specular reflection than in a system with diffuse reflection. For the one-dimensional planar system, the qualitative difference between the angular distribution of the reflected intensity from a specular surface and that from a diffuse surface is illustrated in Fig. 1. The resulting incident intensities to the opposing surface due to these reflections are also shown in the same

Table 1. Comparison between the specular and diffuse reflection results for q_{10} . Values in parentheses are diffuse reflecting results.

ϵ_1	ϵ_2	$w_0 x$	$L = 0.1$	$L = 1.0$	$L = 10.0$
0.3	0.3	-1.0	0.173 (0.173)	0.148 (0.149)	0.064 (0.064)
		0	0.174 (0.174)	0.154 (0.155)	0.076 (0.076)
		1.0	0.174 (0.174)	0.160 (0.161)	0.093 (0.093)
0.3	0.7	-1.0	0.258 (0.258)	0.207 (0.208)	0.072 (0.072)
		0	0.259 (0.260)	0.218 (0.219)	0.088 (0.088)
		1.0	0.261 (0.261)	0.230 (0.232)	0.114 (0.113)
0.3	1.0	-1.0	0.290 (0.290)	0.227 (0.228)	0.075 (0.075)
		0	0.292 (0.292)	0.241 (0.242)	0.092 (0.092)
		1.0	0.294 (0.294)	0.256 (0.257)	0.119 (0.119)

Table 2. Comparison between the specular and diffuse reflection results for q_{50} . Values in parentheses are diffuse reflecting results.

ϵ_1	ϵ_2	$w_0 x$	$L = 0.1$	$L = 1.0$	$L = 10.0$
0.3	0.5	-1.0	0.060 (0.060)	0.490 (0.495)	1.834 (1.853)
		0	0.060 (0.060)	0.509 (0.519)	2.218 (2.243)
		1.0	0.060 (0.061)	0.534 (0.545)	2.806 (2.840)
0.3	0.7	-1.0	0.097 (0.098)	0.782 (0.791)	2.734 (2.757)
		0	0.098 (0.099)	0.825 (0.834)	3.336 (3.366)
		1.0	0.099 (0.100)	0.872 (0.882)	4.278 (4.320)
0.3	1.0	-1.0	0.134 (0.135)	1.052 (1.063)	3.468 (3.485)
		0	0.135 (0.136)	1.115 (1.127)	4.263 (4.285)
		1.0	0.136 (0.137)	1.186 (1.200)	5.531 (5.562)

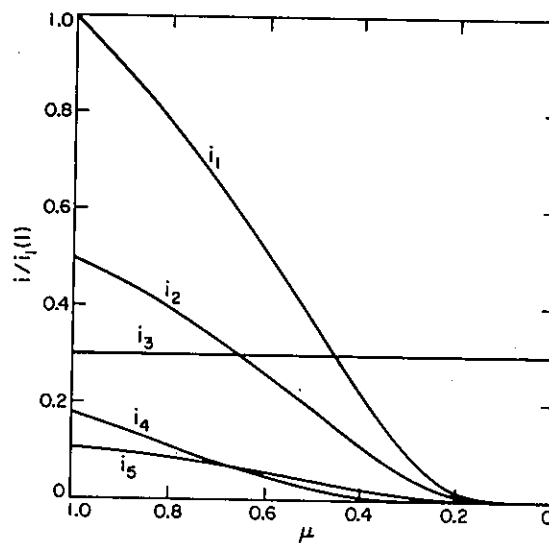


Fig. 1. Comparison of reflection characteristics between a diffuse surface and a specular surface; i_1 = incident intensity [$\exp(-L/\mu)$, $L = 1$]; i_2 = specularly reflected intensity ($\rho = 0.5$); i_3 = diffusely reflected intensity ($\rho = 0.5$); i_4 = incident intensity to the opposing wall due to i_2 ; i_5 = incident intensity to the opposing wall due to i_3 .

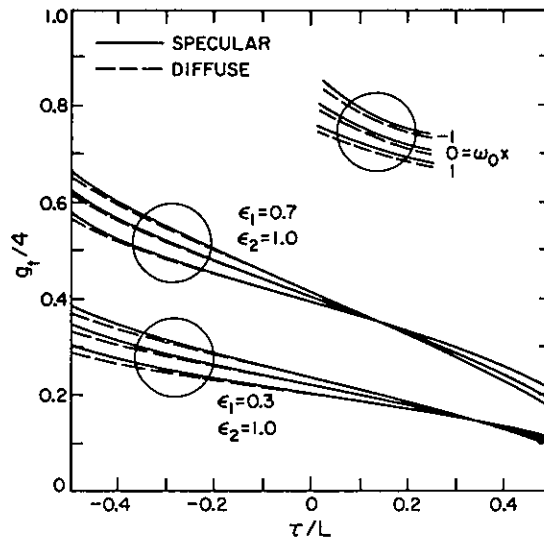
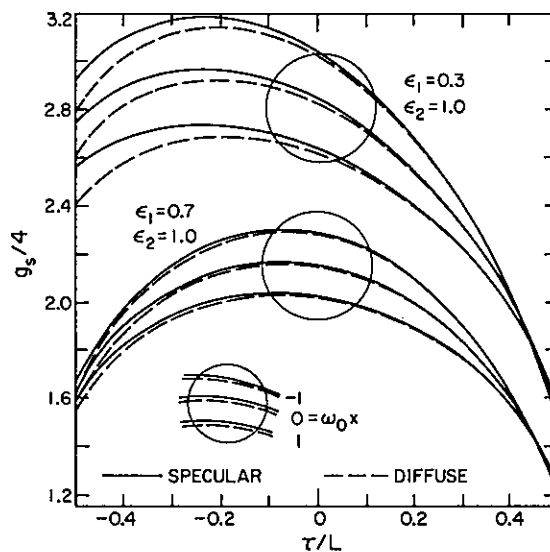
Fig. 2. Comparison between specular and diffuse reflection results for g_t .Fig. 3. Comparison between specular and diffuse reflection results for g_s .

figure. Since the reflected energy from the specular surface concentrates more in the normal direction (at small θ), it traverses on the average a smaller optical path and hence suffers less attenuation. A larger fraction of the reflected energy can thus be transmitted to the opposing surface and there are more multiple reflections. For the case with no heat generation, this effect causes slightly more energy to be reabsorbed by the hotter surface and, therefore, less heat transfer. For the case with heat generation, the energy within the medium is distributed more uniformly among the two surfaces by increased multiple reflection. Since $q_s(-L/2) = q_{s0} - 2L$ and $q_s(L/2) = q_{s0} + 2L$, a smaller q_{s0} with specular reflection means a larger heat transfer to the lower boundary; with $\epsilon_1 \leq \epsilon_2$, this result implies a more uniform heat loss distribution to the two surfaces.

The specular and diffuse reflection results for the temperature profile are presented and compared in Figs. 2 and 3. Again, the difference between the two cases are minor, with the specular case yielding slightly higher temperatures. Numerical results show that this difference is insensitive to the various system parameters (ϵ_1 , ϵ_2 , and $\omega_0 x$) and decreases with increasing optical thickness.

Physically, the preceding results can again be explained by increased multiple reflection for the system with specular surfaces. With unequal wall temperatures and no heat generation,

energy originates mainly from the hot lower wall. The increased multiple reflection and reabsorption of energy by the hot wall means higher absorption for the medium in that region and, therefore, higher temperature as shown in Fig. 2. For equal wall temperature and uniform heat generation, energy originates from within the medium. With increased multiple reflection with specular surfaces, the region near the wall of lower emissivity can see and absorb more of the energy generated. The temperature in that region is thus higher, as shown in Fig. 3.

REFERENCES

1. A. Dyan and C. L. Tien, *J. Heat Transfer* 97C, 391 (1975).
2. W. W. Yuen and L. W. Wong, *J. Heat Transfer* 102, 303 (1980).
3. W. W. Yuen and L. W. Wong, *JQSRT* 22, 231 (1979).
4. J. B. Bergquam and R. A. Seban, *J. Heat Transfer* 93C, 236 (1975).
5. R. D. Cess and A. E. Sotak, *ZAMP* 15, 642 (1964).
6. C. V. Pai, *Appl. Math. and Comp.* 1, 353 (1975).
7. M. S. Özisik and C. E. Siewert, *Int. J. Heat Mass Transfer* 12, 611 (1969).
8. M. A. Heaslet and F. R. Warming, *Int. J. Heat Mass Transfer* 8, 979 (1965).
9. E. M. Sparrow and R. C. Cess, *Radiation Heat Transfer*. McGraw-Hill, New York (1978).